Peptide-Functionalized Gold Nanorods Increase Liver Injury in Hepatitis

Matthias Bartneck,[†,△] Thomas Ritz,[†,△] Heidrun A. Keul,[‡] Mona Wambach,[‡] Jörg Bornemann,[§] Uwe Gbureck,[⊥] Josef Ehling,[∥,¶] Twan Lammers,[∥,#] Felix Heymann,[†] Nikolaus Gassler,[¶] Tom Lüdde,[†] Christian Trautwein,[†] Jürgen Groll,[⊥] and Frank Tacke[†,*]

[†]Department of Medicine III, Medical Faculty, RWTH Aachen, Pauwelsstr. 30, 52074 Aachen, Germany, [‡]DWI e.V. and Institute of Technical and Macromolecular Chemistry, RWTH Aachen, Forckenbeckstr. 50, 52056 Aachen, Germany, [§]Electron Microscopic Facility (EMF), Medical Faculty, RWTH Aachen, Pauwelsstr. 30, 52074 Aachen, Germany, [⊥]Department and Chair for Functional Materials in Medicine and Dentistry, University Hospital Würzburg, Pleicherwall 2, 97070 Würzburg, Germany, [∥]Department of Experimental Molecular Imaging (ExMI), Helmholtz Institute for Biomedical Engineering, Medical Faculty, RWTH Aachen, Pauwelsstr. 30, 52074 Aachen, Germany, [¶]Institute of Pathology, Medical Faculty, RWTH Aachen, Pauwelsstr. 30, 52074 Aachen, Germany, and [#]Department of Targeted Therapeutics, MIRA Institute for Biomedical Technology and Technical Medicine, University of Twente, P.O. Box 217, 7500 AE Enschede, The Netherlands. [△]These authors contributed equally.

ABSTRACT Targeted nanomedicine holds enormous potential for advanced diagnostics and therapy. Although it is known that nanoparticles accumulate in liver *in vivo*, the impact of cell-targeting particles on the liver, especially in disease conditions, is largely obscure. We had previously demonstrated that peptide-conjugated nanoparticles differentially impact macrophage activation *in vitro*.

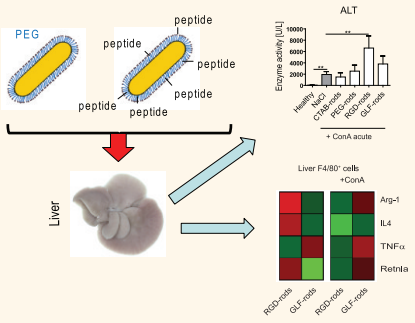

We thus comprehensively studied the distribution of gold nanorods (AuNR) in mice *in vivo* and assessed their hepatotoxicity and impact on systemic and hepatic immune cells in healthy animals and experimental liver disease models. Gold nanorods were stabilized with either cetyltrimethylammonium bromide or poly(ethylene glycol) and additional bioactive tripeptides RGD or GLF. Gold nanorods mostly accumulated in liver upon systemic injection in mice, as evidenced by inductively coupled plasma mass spectrometry from different organs and by non-invasive microcomputerized tomography whole-body imaging. In liver, AuNR were only found in macrophages by seedless deposition and electron microscopy. In healthy animals, AuNR did not cause significant hepatotoxicity as evidenced by biochemical and histological analyses, even at high AuNR doses. However, flow cytometry and gene expression studies revealed that AuNR polarized hepatic macrophages, even at low doses, dependent on the respective peptide sequence, toward M1 or M2 activation. While peptide-modified AuNR did not influence liver scarring, termed fibrosis, in chronic hepatic injury models, AuNR-induced preactivation of hepatic macrophages significantly exacerbated liver damage and disease activity in experimental immune-mediated hepatitis in mice. Bioactively targeted gold nanoparticles are thus potentially harmful in clinically relevant settings of liver injury, as they can aggravate hepatitis severity.

KEYWORDS: nanomedicine · macrophages · peptide-functionalized nanoparticles · liver injury · Concanavalin A · liver fibrosis

Gold nanorods (AuNR) represent a relatively novel class of nanoparticles that hold significant potential for many areas of medicine, including for diagnostic and drug delivery purposes.[1] AuNR synthesis and surface functionalization is well-established including the possibility to tailor their size and shape. Moreover, their unique interaction with light and the fact that gold is not naturally occurring in living organisms allows precise localization and quantification of gold nanoparticles. All these points make gold nanoparticles ideal candidates as model particles for systematic studies on the effects of nanoparticles *in vivo*. While most research today is focused on achieving active targeting and therapeutic advantage of nanoparticles by chemical modifications, such as attachment of short peptide sequences, the effects of nanosystems bearing targeting molecules on the whole body, especially in clinically relevant settings of disease, are largely unknown.

The liver is the key organ for determining the fate of nanoparticles larger than 8 nm that do not undergo glomerular filtration.[2] Yet, very limited studies focused on the effects of engineered nanoparticles on liver, especially considering healthy and diseased tissue. Potential effects of nanotherapeutics on hepatic diseases are consequential because around 500 million people are chronically infected with hepatitis B or C virus worldwide,[3] being rendered at high risk for developing chronic scarring of the liver (fibrosis), which might later progress into cirrhosis or hepatocellular carcinoma.[4] Furthermore, in the U.S., more than 20% of the general population, with a constantly increasing incidence rate, suffers from obesity[5] and is thereby at high risk for non-alcoholic fatty liver disease. Given the high prevalence of viral hepatitis or liver fibrosis and cirrhosis in humans, systemic administration of engineered nanoparticles might impact the course and outcome of liver diseases *in vivo*.

Independent of nanoparticle surface chemistry, usually a high percentage of nanoparticles

* Address correspondence to frank.tacke@gmx.net.

Received for review June 6, 2012 and accepted September 20, 2012.

Published online September 21, 2012
10.1021/nn302502u

injected into the bloodstream is cleared by the liver, mainly by the liver resident macrophages that constitute 80−90% of all macrophages of the body.[6] Importantly, peptide-conjugated nanoparticles have been previously shown to induce macrophage activation *in vitro*.[7] A nanoparticle-induced activation of macrophages might be particularly relevant in the context of liver diseases because macrophages were found to promote hepatic fibrosis progression by releasing cytokines and activating collagen-producing hepatic stellate cells[8] and potentially also exacerbate hepatitis.[9] Macrophages are a heterogeneous population of phagocytic cells that is often characterized as polarized into rather pro-inflammatory M1 or anti-inflammatory M2 macrophages. In mice, M1 cells express among others the tumor necrosis factor α (TNFα), inducible nitric oxide synthase (iNOS), and interleukin 1β (IL1β), whereas M2 cells typically express Arginase 1 (Arg1), resistin-like alpha (Retnla, FIZZ-1), and IL4.[10] Murine pro-inflammatory macrophages in the liver derive from circulating monocytes that migrate into the liver upon injury and express F4/80, CD11b, and the Ly6C antigen, whereas Kupffer cells represent resident liver macrophages expressing high levels of F4/80 but low levels of Ly6C and CD11b on their surface.[9] In accordance to variations in Ly6C antigen expression,[11] murine hepatic macrophages differentially express alternative activation markers, specifically the IL4 receptor α (CD124). The IL4-based signaling is essential to protect from organ injury and to inhibit inflammation in disease.[12] Additional murine M2 surface markers are the mannose receptor (CD206) and the macrophage C-type lectin domain family 10, member A (CLEC10A, CD301).

As novel nanoparticle-based treatment options might be applied in clinical settings of multimorbidity, we decided to comprehensively study the distribution of AuNR *in vivo* and assess their overall toxicity and their impact on systemic and hepatic immune cells. In this study, we assessed the concentration-dependent uptake of gold nanorods into five different major organs, liver, spleen, lung, kidney, and brain, after 24 h using inductively coupled plasma mass spectrometry (ICP-MS). Further, we established a non-invasive screening method that is based on microcomputed tomography (μCT) for longitudinal measurements of gold nanoparticle *in vivo* distribution. We studied the effects of gold nanorods on important blood cell types, liver injury, as reflected by serum alanine aminotransferase (ALT) levels, and serum cytokine release in otherwise healthy mice. To determine effects on liver histology, we analyzed liver sections using immunohistochemistry. Transmission electron microscopy was done to assess cell-type-specific accumulation. We compared effects of the nanoparticles on liver resident and infiltrating macrophages, as well as on other hepatic immune cell populations. For assessing the effects of PEGylation and additional modification with bioactive peptides on the progression of liver disease, we generated gold nanorods stabilized with cetyltrimethylammonium bromide (CTAB), polyethylene glycol (PEG), and with the bioactive tripeptides RGD and GLF attached to the PEG layer. In order to investigate effects in the context of chronic liver injury *in vivo*, 8 weeks old C57BL/6 mice were respectively treated with hepatotoxic carbon tetrachloride (CCl_4) as well as with nanoparticles for 6 weeks, and the animals were subsequently analyzed for their development of scarred tissue (fibrosis). Acute immune-mediated hepatitis was induced in nanorod-treated animals by injection of Concanavalin A (ConA) in mice. Hepatic macrophages were isolated from liver and analyzed for their expression of genes that are characteristic for a certain phenotype of macrophages.

RESULTS AND DISCUSSION

In order to investigate a potential hepatotoxicity of AuNR on healthy animals *in vivo*, we first assessed AuNR biodistribution upon intravenous injection into five major organs of mice using ICP-MS. It appeared that CTAB-capped AuNR predominantly accumulated in liver (Figure 1a), followed by spleen and, at the highest concentration, also lung. At the highest concentration of 1200 μg/kg mice body weight, a macroscopically visible brownish discoloration of explanted livers was visible (Figure 1b). Seedless deposition (size enhancement) of gold in liver and spleen sections confirmed AuNR accumulation in these organs, in cells of the reticuloendothelial system (Figure S1 in the Supporting Information). As a non-invasive approach to study particle distribution *in vivo*, whole-body μCT was performed. Mice were scanned 1 and 6 days after intravenous injection of different doses of CTAB-coated gold nanorods (12, 120, and 1200 μg/kg body weight) and isotonic saline solution (0.9% NaCl) as control. These studies showed an increased accumulation in liver compared to spleen (intermediate) and kidney (very low) and thus confirmed the predominant accumulation of AuNR in liver, reflected by a distinct contrast enhancement comparing saline and AuNR-treated mice (Figure 2a,b and Figure S2). Moreover, it has to be kept in mind that the dry weight of the liver is approximately 50 times higher than of spleen (Figure S3), corroborating that the liver is the major organ for gold nanorod accumulation *in vivo*. After 6 days, the nanoparticles were still detectable in the liver at similarly high levels (Figure 2c,d and Figure S4), clearly evident upon quantification of the gold intrinsic radiodensity (Figure 2e,f). This suggests a predominant hepatic accumulation, a low level of hepatobiliary clearance, and a prolonged persistence of AuNR in the liver *in vivo*.

To determine histological changes in liver morphology due to the presence of AuNR, we prepared tissue sections and performed hematoxylin and eosin (H&E) staining. AuNR administration did not provoke overt

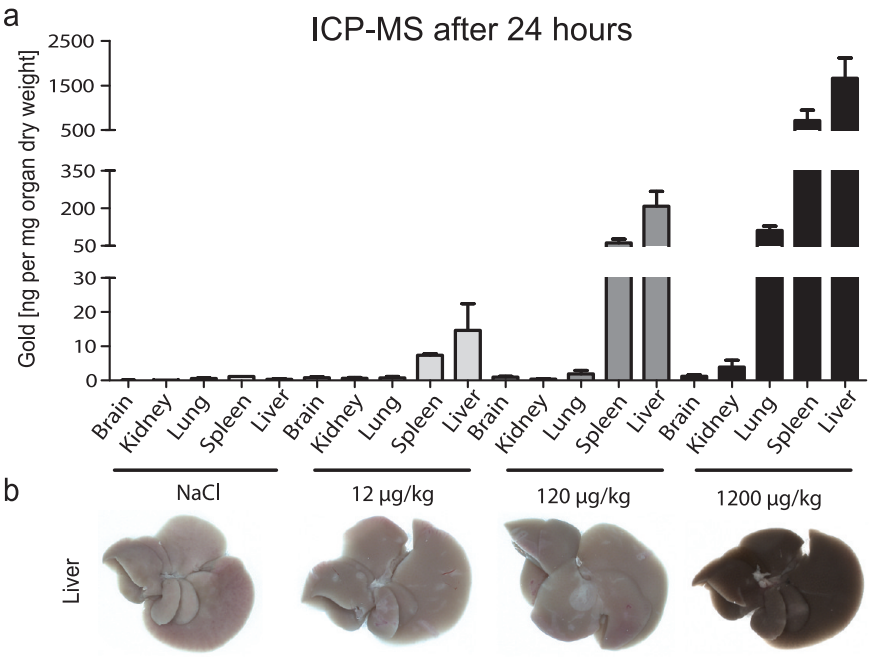

Figure 1. AuNR distribution *in vivo*. NaCl (control) or CTAB-coated AuNR (concentration given as μg/kg body weight) were injected intravenously into 8−12 week old C57BL/6 wild-type mice that were sacrificed after 24 h (n = 6 mice per condition). Inductively coupled plasma mass spectrometry (ICP-MS) data on the distribution of gold nanorods in different organs, normalized to dry organ weight (a). Macroscopic appearance of the liver (b).

tissue damage in liver histology, although some inflammatory leukocytes were noted around the hepatic portal fields at high doses of AuNR. We found a mild increase in cells located in the sinusoidal space that we hypothesized to be macrophages (Figure 3a,b). To prove that the nanoparticles were located in macrophages, we conducted transmission electron microscopy (TEM) and could show that the rods were located in hepatic macrophages but not in parenchymal cells (hepatocytes) or endothelial cells of the liver (Figure 3b). The unexpected lack of nanorod uptake by endothelial cells, as reported by others,[13] might be explained by sedimentation effects that exist *in vitro* but are strongly decreased *in vivo* due to constant flow conditions; however, we cannot exclude that endothelial cells had transiently carried nanorods, which were not detectable anymore at 24 h after injection. Studies on other organs based on TEM showed that also in spleen AuNR were located in macrophages (Figure S5).

To study potential systemic effects of nanorods, we performed flow cytometric analyses of blood cells in order to unravel any changes associated with blood leukocytes. At the highest AuNR concentration, inflammatory phagocytic blood cells, namely, neutrophils and monocytes, increased mildly (Figure 4a), and the numbers of pro-inflammatory Ly6C^{high} monocytes circulating in blood were increased at the highest AuNR dose (Figure S6). We additionally studied other important blood immune cells such as T cells, B cells, natural killer (NK) cells, natural killer T cells (NKT cells), and cytotoxic CD8 cells. Notably, none of these other immune cells were significantly affected in the circulation (Figure S6). CTAB-stabilized AuNR, which are known to be toxic *in vitro*,[14] surprisingly only mildly increased ALT (a sensitive indicator for hepatocellular injury) enzyme activity *in vivo* (Figure 4b) and did also not induce significantly elevated levels of inflammatory cytokines in serum (Figure 4c).

Upon disease or stress stimuli, immune cells migrate from blood to organs. Immune cell infiltration into the liver therefore indicates very early inflammatory activation. In order to detect even mild hepatic inflammatory responses upon nanorod administration, extensive flow cytometric analyses were conducted. In liver, infiltrating inflammatory macrophages (iMΦ; CD11b$^+$ F4/80$^+$)[8] as shown in Figure 5a accumulated significantly at the highest concentration of nanorods, whereas the resident Kupffer cell (KC; CD11b$^-$ F4/80$^+$) macrophage population as well as neutrophils were not significantly affected (Figure 5a,b), similar to other hepatic immune cells (Figure S7). Blood monocytes and the hepatic macrophage populations iMΦ and KC exhibit characteristic differences in their expression of the Ly6C antigen; Ly6C expression is highest on circulating (Ly6C^{high}) monocytes, is decreased on monocyte-derived hepatic iMΦ upon migration into organs such as liver, and is low to negative on tissue-resident macrophages such as KC (Figure S8).[8]

Earlier studies have simplified the hepatic macrophage pool as being KC without differentiating between infiltrating subsets, mainly iMΦ, and of resident macrophages, KC in the more specific sense.[15] To address the question whether hepatic macrophages differ in their efficiency of AuNR uptake, we isolated

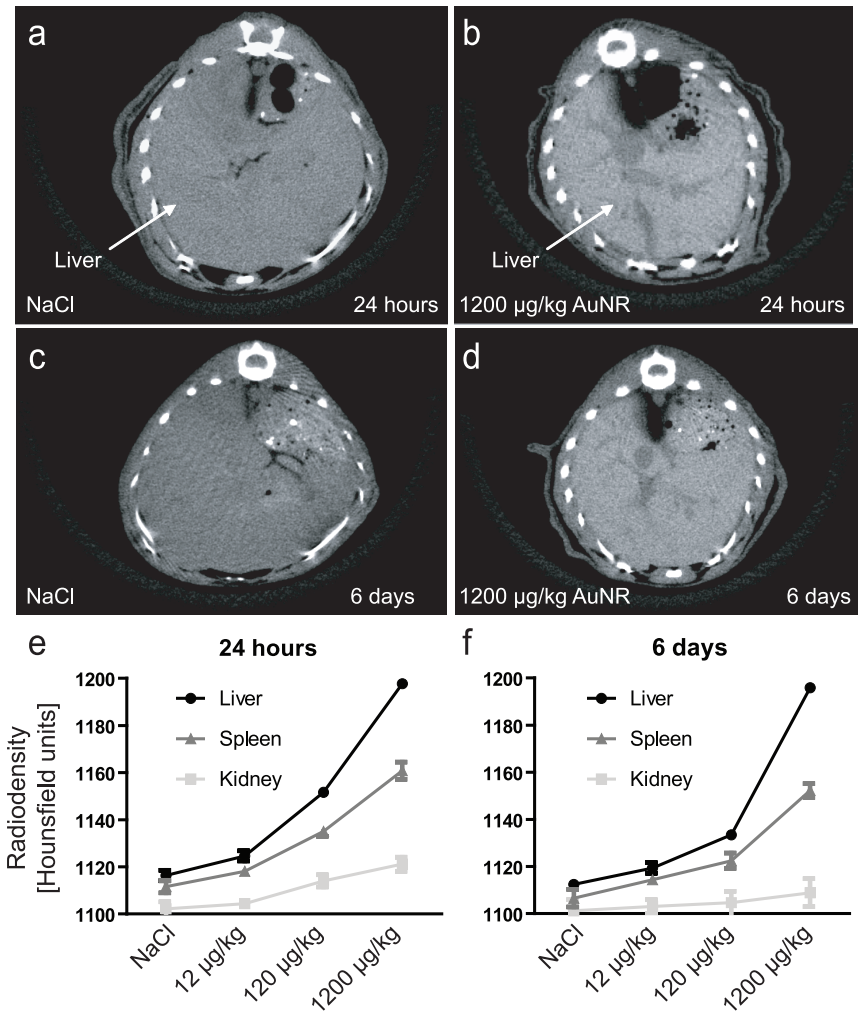

Figure 2. Non-invasive monitoring of AuNR distribution *in vivo*. Microcomputed tomography scans after 24 h of injection of saline (a) or 1200 μg/kg AuNR (b), analyzed using identical imaging settings. The contrast of the liver is enhanced due to AuNR deposition. After 6 days, data appear similar for saline (c) or AuNR treatment (d). Statistical summary of radiodensity quantification after 24 h (e) or 6 days (f) given as Hounsfield units in liver, kidney, and spleen.

iMΦ and KC from mice 24 h after the injection of 120 μg/kg CTAB-coated AuNR using fluorescence-activated cell sorting and quantified the uptake of AuNR by the distinct macrophage subsets using ICP-MS. The iMΦ internalized an almost 30-fold larger amount of nanoparticles per cell (Figure S9). These data show that there is a high necessity to discriminate macrophage subsets in the liver, as the iMΦ is believed to primarily mediate pro-inflammatory effects in conditions of liver injury.[8]

The activation profiles of hepatic macrophages, as reflected by the surface markers CD124, CD206, and CD301, were only mildly affected by gold nanorods (Table S1 and Figure S10). Earlier *in vitro* studies with human macrophages had shown that significant changes in surface marker expression appear as late as after 7 days and that gene regulation is already affected after only 1 day.[16] We also performed gene expression studies of liver tissue samples and found that Retnla transcript abundance, which is believed to exert inflammation-limiting properties,[17] increased with nanorod concentration. Similarly, up-regulation of the macrophage receptor with collagenous structure (Marco) at the highest AuNR dose might be related to macrophage particle uptake as this scavenger receptor is involved into the uptake of unopsonized particles[18] and also limits inflammation.[19] Further, interleukin 4 (IL4) was up-regulated by the two highest doses of AuNR, which might be a secondary effect of the particles as IL4 is expressed by activated T cells.[20] The IL4 receptor (IL4R)−IL4 axis was also reported to down-regulate inflammation.[12] Expression of IL1β, the key molecule for stress sensing by the immune system,[21] was only triggered at the highest dose of AuNR (Figure S11).

Cytokine protein profiling showed that, even at the highest concentration of nanorods, there were only low levels of the pro-inflammatory cytokines CXC-chemokine ligand 1 (CXCL1), interleukin 6 (IL6), and CC-chemokine ligand 2 (CCL2) in the liver (Figure 5c). Collectively,

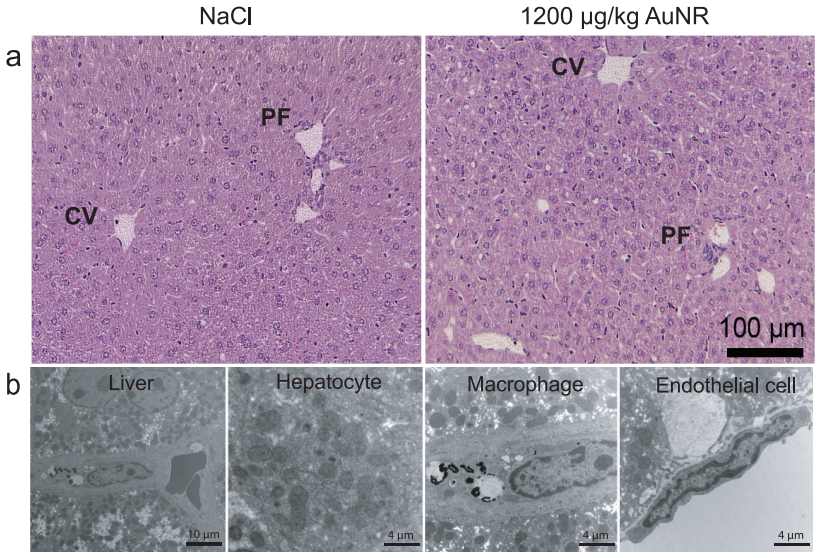

Figure 3. Gold nanorods in healthy liver. CTAB-coated AuNR (concentration given as μg/kg body weight) were injected intravenously into 8−12 week old C57BL/6 wild-type mice that were sacrificed after 24 h. Liver morphology and accumulation in hepatic macrophages. Hematoxylin eosin staining of liver sections without treatment and after treatment with 1200 μg/kg AuNR (a). In the liver structure, the central vein (CV) and portal fields (PF) are marked. A discrete increase of inflammatory cells (small round blue cells) can be noted in periportal regions and sinusoidal space. In the liver, nanorods (black dots) accumulate in macrophages but not in hepatocytes or endothelial cells, as shown by transmission electron microscopy of ultrathin liver sections (b).

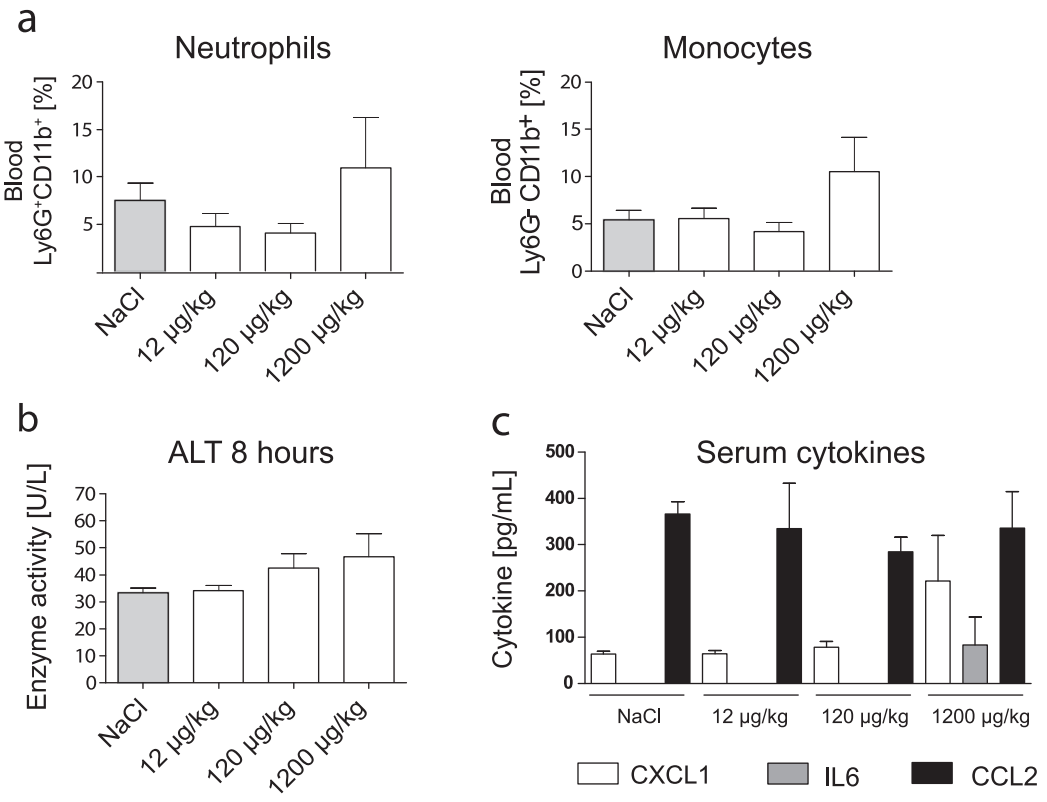

Figure 4. Toxicity and blood immune cell alterations by AuNR *in vivo*. Eight week old C57BL/6 mice were injected intravenously with NaCl (control) or different concentrations of CTAB-coated AuNR (concentration given as μg/kg body weight). Mice were sacrificed after 24 h (n = 6 mice per condition). Flow cytometric analysis of circulating monocytes and neutrophils (a). Hepatic injury was determined by serum alanine transaminase (ALT) activity (b). Cytokine profiling (protein levels) in serum (c). Data represent mean ± SD; *P < 0.05 (unpaired Student's t test).

these data suggest that CTAB-coated AuNR are—over a wide dose range—neither hepatotoxic nor immunotoxic in healthy mice *in vivo*, unanticipated from *in vitro* studies.[14] However, at high doses of gold

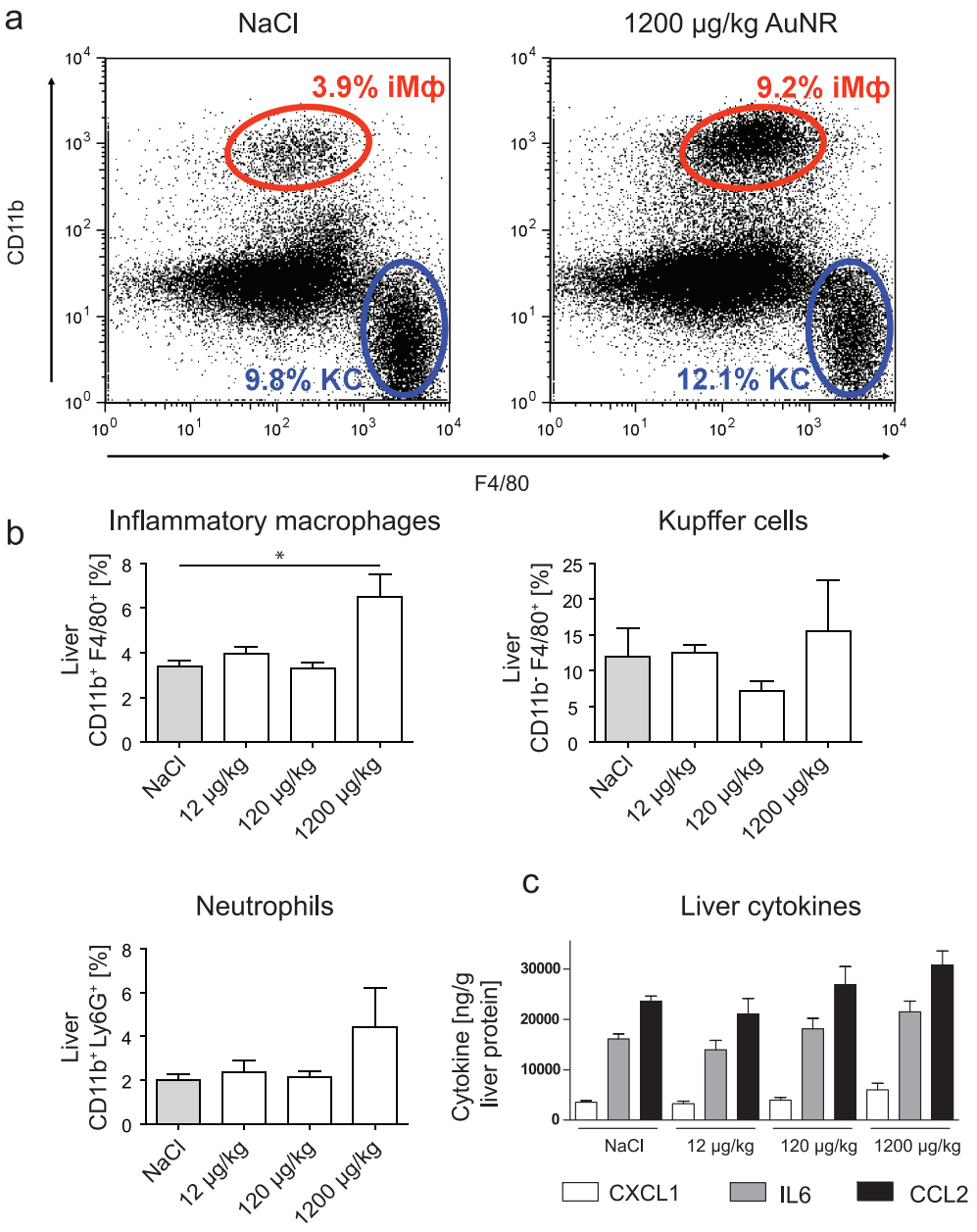

Figure 5. Liver immune cell number alterations by AuNR *in vivo*. Eight week old C57BL/6 mice were injected intravenously with different concentrations of CTAB-coated AuNR (concentration given as μg/kg body weight). Mice were sacrificed after 24 h ($n = 6$ mice per condition). Representative flow cytometric scatter plots of intrahepatic macrophages: inflammatory macrophages (iMΦ) or resident Kupffer cells (KC) (a). Statistical summary of flow cytometric analysis of intrahepatic neutrophils, iMΦ, or KC (b). Cytokine profiling (protein levels) in liver (c). Data represent mean ± SD; *$P < 0.05$ (unpaired Student's *t* test).

nanorods, alterations of the composition of the hepatic macrophage subsets as well as of macrophage polarization markers were noted, specifically up-regulation of key molecules of M2 macrophage activation. This prompted us to address whether gold nanorods might affect the outcome of liver injury *in vivo*.

We next examined the effects of different biofunctionalized AuNR in conditions of chronic liver injury in a mouse model that reflects chronic disease progression in humans. Hepatic injury and fibrosis were experimentally induced by challenging mice for 6 weeks twice weekly with the hepatotoxic agent CCl_4. AuNR were injected weekly at a dose of 12 μg/kg. Fibromodulatory effects of AuNR capped either with CTAB, PEG, or the bioactive tripeptides GLF or RGD were comprehensively compared (a scheme of the different particles is shown in Figure 6a). The peptide sequence RGD is considered tumor-binding,[22] and GLF is thought to be macrophage-binding.[23] Importantly, all peptide-functionalized gold nanorod formulations did not induce hepatotoxicity, as assessed by biochemical and histological analyses in naïve animals at this dose, similar to the findings from CTAB rods (Figure S12).

CTAB-coated nanorods did not alter the outcome of chronic liver injury, whereas GLF- and RGD-capped

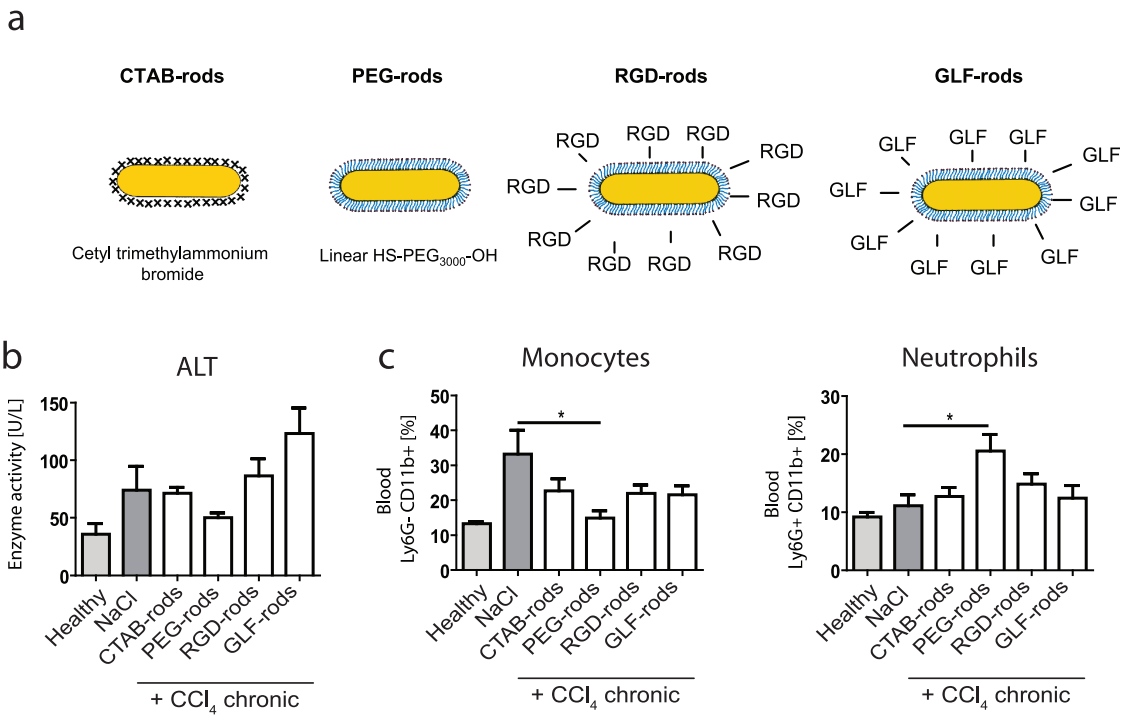

Figure 6. Effects of biofunctionalized nanorods on blood cells in liver fibrosis *in vivo*. Four different types of gold nanorods were tested in chronic toxic liver injury, those stabilized with CTAB, with PEG, with the RGD tripeptide, or with the GLF tripeptide (a). Chronic toxic liver injury was induced by 6 weeks of carbon tetrachloride (CCl_4) treatment in C57BL/6 mice (n = 6 mice per condition). Nanorods were administered weekly at 12 μg/kg. Mice were sacrificed after 6 weeks of CCl_4 challenge, 48 h after the last injection. Hepatic injury was determined by serum alanine transaminase activity (ALT) (b). Flow cytometric analysis of peripheral blood circulating leukocytes including monocytes and neutrophils (c). Data are expressed as mean ± SD; *P < 0.05, ***P < 0.001 (unpaired Student's t test).

particles led to modestly increased ALT levels (Figure 6b). Interestingly, PEG rods led to a significant decrease in blood monocytes and to an increase in neutrophils (Figure 6c), which is likely related to the increased circulation half-life of PEG-coated nanoparticles.[24] This demonstrates immunomodulatory activity of nanoparticles also *in vivo* that is based on AuNR uptake and subsequent intracellular actions on immune cell activation.[16] Again, all other studied circulating immune cells were unaffected (Figure S13).

The degree of fibrosis is reflected by the deposition of collagen in the extracellular matrix of the liver. Sirius Red staining of collagen revealed that mice in all groups developed significant liver fibrosis (Figure 7a). Quantification of collagen fiber formation based on Sirius Red staining as well as hepatic hydroxyproline concentration as an independent measure of fibrosis progression revealed no significant differences in fibrosis development by the different particle stabilizers (Figure S14). Hepatic immune cell numbers were mostly unaffected by nanorods, except for significantly decreased NK cells in the livers treated with CTAB, RGD, and GLF rods (Figure 7b and Figure S15). These effects on NK cells are hypothesized to be secondary effects of the liver injury process as they are involved in eliminating injured cells and, like all lymphocytes, do not internalize these nanoparticles as proven by earlier *in vitro* studies.[16]

Interestingly, we noted that, in liver fibrosis, the macrophage surface markers CD124, CD206, and CD301, which have been linked to fibrogenic properties in nonhepatic models,[25−27] were distinctly altered by AuNR in chronic injury models based on their chemistry, especially by PEG rods; they significantly decreased expression of the IL4R by KC, whereas these particles in parallel increased CD206 expression by iMΦ. RGD rods significantly decreased the number of CD206 expressing iMΦ (Table S2 and Figure S16). Taken together, the different nanorods displayed remarkable immunomodulatory effects in macrophages that are most pronounced in disease conditions.

In addition to the long-term effects of nanomaterials on fibrosis development, they might also affect the outcome of acute immune cell-mediated liver disease such as hepatitis. We have previously demonstrated that distinct biofunctionalized AuNR impact the polarization of human macrophages *in vitro*.[16] To better delineate possible consequences of these particles in the setting of hepatitis, we applied the well-established mouse model of experimental hepatitis induced by the lectin ConA which results in severe liver injury within 8 h. Strikingly, in mice suffering from hepatitis, pretreatment with both peptide-terminated AuNR led to larger areas of necrotic hepatocytes and to an increased infiltration by mononuclear cells in histology (Figure 8a). In line

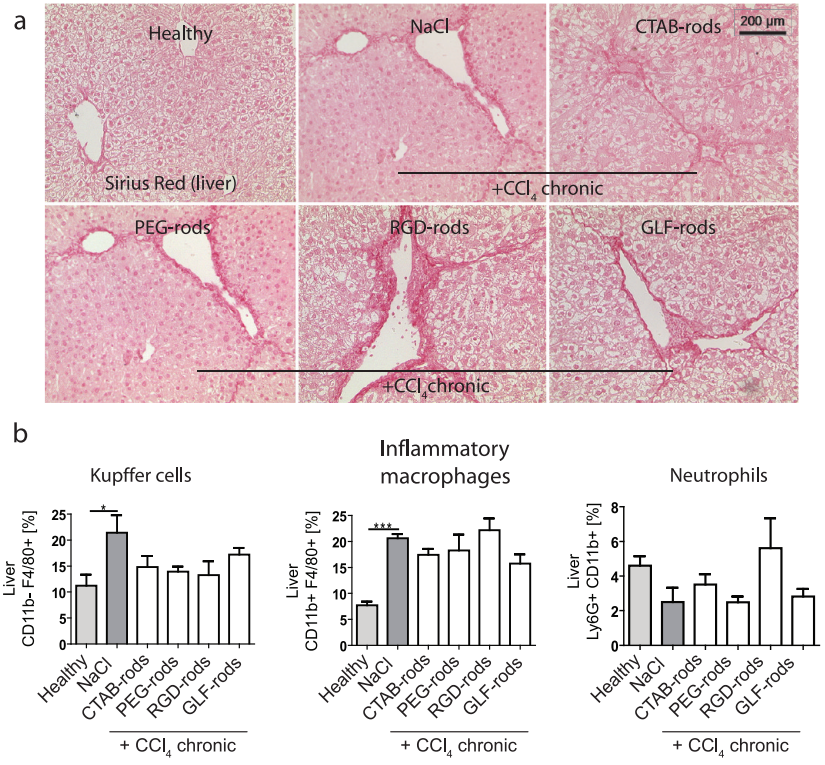

Figure 7. Effects of biofunctionalized nanorods on liver fibrogenesis *in vivo*. Chronic toxic liver injury was induced by 6 weeks of carbon tetrachloride (CCl_4) treatment in C57BL/6 mice (n = 6 mice per condition). Representative micrographs of liver fibrosis scoring based on Sirius Red staining, collagen-rich scar tissue appears red (a). Flow cytometric analysis of liver macrophage subsets and neutrophils (shown as percent of CD45 expressing hepatic leukocytes) (b). Data are expressed as mean ± SD; *P < 0.05, ***P < 0.001 (unpaired Student's t test).

with these observations, ALT serum levels after ConA treatment were significantly increased by RGD-coated rods, reflecting increased liver injury by RGD-capped rods. GLF rods also accelerated liver injury, but the increase in ALT levels did not reach statistical significance (Figure 8b). The number of liver macrophages (iMΦ and KC) was only weakly affected in response to the different nanorods (Figure 8c). Frequencies of other blood cells (Figure S17) could not be linked to the extent of liver injury. In liver, NK and CD8 cells were significantly increased by PEG rod treatment (Figure S18). As mentioned above, these are hypothesized to be rather indirect effects of the nanoparticles, as NK and CD8 cells do not directly interact with the AuNR.[16]

On the basis of the preferential accumulation of AuNR in hepatic macrophages (Figure 3b) *in vivo* and their influence on macrophage functions *in vitro*,[28] we next studied the impact of differently functionalized nanorods on hepatic macrophage polarization in acute hepatitis by flow cytometry. Nanorod surface chemistry distinctly impacted the phenotype of hepatic macrophages in the ConA hepatitis model, as PEG rods induced a significant up-regulation of CD124 by KC (Table S3 and Figure S19). The differences in the expression of the IL4R (CD124) in both liver injury models (Tables S2 and S3) might be explained by the different molecular mechanisms accounting for the liver injury that are induced by ConA or CCl_4. CCl_4-mediated injury is based on hepatocyte death,[29] and inflammation is a secondary effect, whereas the ConA model represents immune cell-mediated liver damage, mainly by macrophages and T cells.[30] To further characterize the activation profile of hepatic macrophages triggered by RGD or GLF-capped nanorods, we performed gene expression studies of whole liver extracts and of isolated F4/80$^+$ hepatic macrophages from control and ConA-injured livers that had been pretreated with RGD or GLF-capped nanorods. In whole liver specimens treated with nanorods only, gene expression levels of Arg1, IL4, and TNFα were found to be slightly reduced, except for a weak up-regulation of IL4 by GLF rods. Retnla was up-regulated by RGD rods under both conditions (Figure 9).

Strikingly, isolated hepatic macrophages from non-injured livers expressed high levels of Arg1, IL4, and Retnla but low levels of TNFα upon RGD rod administration (Figure 9), clearly indicating an alternatively activated macrophage polarization (M2 cells). M2 cell activation has been linked to anti-inflammatory cytokine production but is also a response in means to suppress tissue injury in allergic or helminth inflammation.[31,32] GLF rods, on the other hand, polarized hepatic macrophages toward the M1 subtype linked to inflammatory injuries such as bacterial infections,[33] as evidenced by reduced levels of

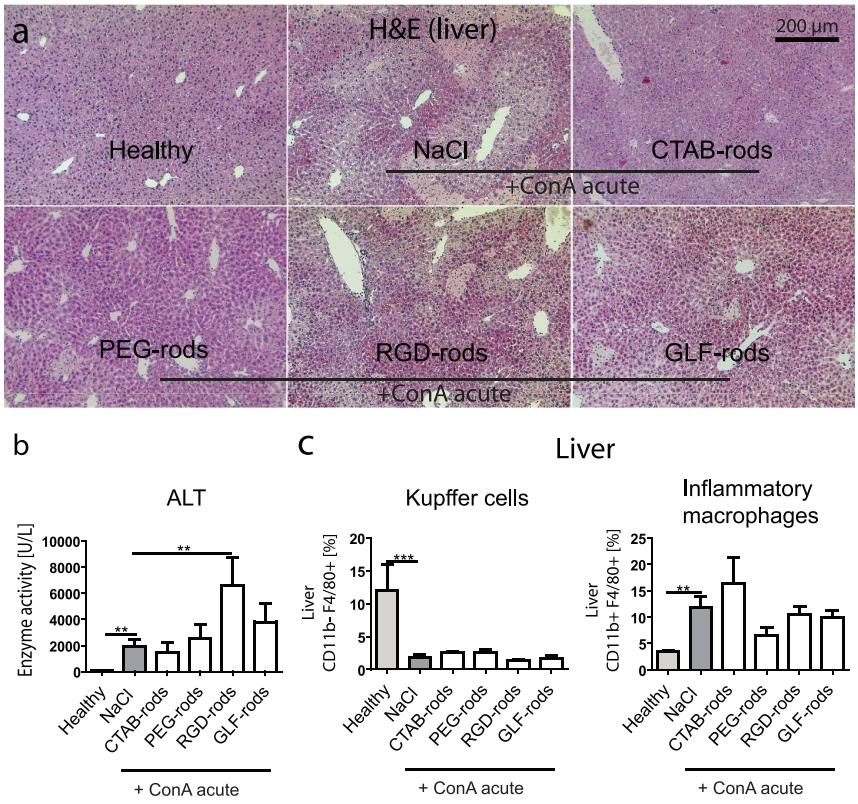

Figure 8. Peptide-functionalized nanorods in acute hepatitis. Eight week old C57BL/6 mice were treated with different biofunctionalized gold nanorods intravenously, followed 40 h later by intravenous injection of 15 mg/kg Concanavalin A (ConA). Mice (n = 6 per condition) were sacrificed 8 h after ConA injection. Hematoxilin eosin staining of liver sections. Please note necrotic areas (lighter) and infiltration of mononuclear cells (small dark blue spots) (a). Alanine transaminase activity (ALT) in serum as a measure of liver injury (b). Flow cytometric analysis of liver leukocytes, KC and iMΦ (c). Data are shown as mean ± SD, normalized to sodium-chloride-treated control animals; **P < 0.005 and ***P < 0.001 (unpaired Student's t test).

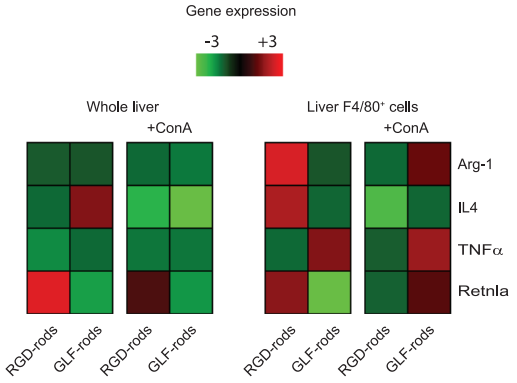

Figure 9. Effects of peptide-functionalized nanorods on intrahepatic macrophage gene expression in acute hepatitis. Eight week old C57BL/6 mice were treated with different biofunctionalized gold nanorods intravenously, followed 40 h later by intravenous injection of 15 mg/kg Concanavalin A (ConA). Mice were sacrificed 8 h after ConA injection. Gene expression levels for macrophage polarization are shown for either whole liver or hepatic macrophages. Data represent mean values of n = 3.

Arg1, IL4, and Retnla but increased TNFα (Figure 9). In both cases, the hepatic macrophages reverted their gene expression profile in ConA-induced hepatitis; RGD rods led to an apparently distinct state of both M1 and M2 marker down-regulation, whereas GLF rods led to a weak up-regulation of two M2 markers (Arg1 and Retnla) and of the M1 marker TNFα but also to down-regulation of IL4 (Figure 9). The reason for the differential changes in macrophage activation might be interactions of the biofunctional peptides inside the cells with specific inflammatory pathways. In fact, it has been shown earlier that peptide conjugation to nanoparticles affects macrophage activation upon uptake of these particles.[7] Using identically generated RGD and GLF rods, we have previously demonstrated that these peptide-modified AuNR influence the polarization of human macrophages *in vitro*.[28]

Collectively, our data convincingly show that modifying the surface chemistry of gold nanoparticles can considerably affect the polarization and functionality of inflammatory macrophages and Kupffer cells in the liver, resulting in a preactivation state that promotes increased susceptibility to acute inflammatory injury. ConA-induced hepatitis is widely used as an experimental model for acute hepatitis, as this *Canavalia ensiformis* mitogen with carbohydrate-binding (lectin) properties causes a vigorous $CD4^+$ T-cell stimulation, resulting in TNFα-related hepatic necrosis after a single administration.[30] It is well-known that this model, like human liver diseases,[9] crucially depends on the activation of hepatic macrophages and liver injury can

be significantly inhibited by depleting macrophages in experimental conditions.[34]

CONCLUSIONS

Immunomodulatory effects of nanomaterials can be strongly amplified under disease conditions, possibly due to additive effects of nanoparticles and the underlying disease on immune cells and specifically macrophage activation. Using specific gold nanorod formulations as a model system, our study suggests that the prepolarization of hepatic macrophages induced by specific nanoparticles, in our case peptide-functionalized particles, either toward so-called M1 or M2 polarized macrophages, can significantly exacerbate liver injury in acute hepatitis. The μCT data after 6 days further suggest that AuNR may persist within the liver for a long time period *in vivo*, and future studies should outline their long-term fate especially regarding interactions with immune cells. Further studies are required to clarify to which extent these observations on nanotoxicity apply to different particle classes. The use of cell-targeting nanoparticles in novel nanomedicine-based therapies, however, requires particular caution, especially if liver diseases are concomitantly present.

METHODS

Nanoparticle Synthesis, *In Vivo* Distribution, and Quantification. AuNR were synthesized based on the seed-growth strategy, and ligand exchange of CTAB against PEG was performed as reported earlier.[16,28] In addition, the tripeptides RGD and GLF were attached to PEG-coated nanorods, and particles were analyzed as demonstrated recently.[28] The enlargement of gold nanoparticles up to the microscale was performed by electroless deposition of gold nanorods in cryosections of organs using the GoldEnhance LM Kit 2112 (Nanoprobes, New York, USA) followed by eosin staining. Cells were prepared for transmission electron microscopy as described earlier.[16] ICP-MS was performed to quantify the intracellular quantity of gold as done before.[28]

Mice. C57BL/6 wild-type mice were housed in a specific pathogen-free environment. All experiments were done with male animals at 8−12 weeks of age under ethical conditions approved by the appropriate authorities according to German legal requirements. The amount of gold injected intravenously into mice was adapted from *in vitro* studies with human primary cells (see Supporting Information section 9 for details).

Microcomputed Tomography. For *in vivo* imaging and quantification of particle distribution non-invasive μCT was performed. We used a gantry-based dual-energy microcomputed TomoScope 30s Duo (CT-Imaging, Erlangen, Germany). Mice were anaesthetized using 1.5% isofluorane inhalation narcosis. For the duration of the scan, mice were breathing spontaneously *via* a mask. We performed a dual-energy scan at 41 and 65 kV (0.5 and 1 mA), acquiring 2880 projections of size 1032 $\times$ 1024 over 6 min of continuous rotation. Images were reconstructed using a Feldkamp type reconstruction (CT-Imaging, Erlangen, Germany) that generates a voxel size of 70 $\times$ 70 $\times$ 70 μm^3. Subsequently, images were analyzed using amide.[35] Three different regions of interest (ROI) for liver (3 $\times$ 3 x 3 mm^3) as well as for spleen and kidney (1.5 $\times$ 1.5 $\times$ 1.5 mm^3) were scanned using identical settings for each organ, and the mean of the brightness (Hounsfield units) within the ROI was evaluated per organ for each mouse at days 1 and 6. Three-dimensional architecture was visualized using 3D volume rendering software MeVisLab (MeVis Medical Solutions AG, Bremen, Germany).

Induction of Acute or Chronic Liver Injury. To study the effects of gold nanorods in liver injury models, nanorods were adjusted to the desired dose in sodium chloride (NaCl) and administered intravenously at 12 μg/kg body weight. After 40 h, ConA (Sigma-Aldrich, St. Louis, MO, USA) was administered intravenously at 15 mg/kg, and 8 h later, mice were sacrificed. Control animals received sodium chloride instead of nanoparticles. For chronic liver injury, mice were injected twice weekly with 0.6 mL/kg body weight CCl_4 (Merck, Darmstadt, Germany) intraperitoneally, dissolved in corn oil, for 6 weeks. Control animals received the same volume of vehicle (corn oil). Mice were sacrificed 48 h after the last injection.

Liver Enzymes, Histology, and Immunohistochemistry. ALT was determined at 37 °C in serum using the Modular Preanalytics System (Roche, Penzberg, Germany). H&E and Sirius Red stainings were conducted according to established protocols. Sirius Red stained pictures were analyzed by area fraction quantification (ImageJ) in a blinded fashion.[8]

Isolation and Flow Cytometric Analysis of Blood and Intrahepatic Leukocytes. Blood was gained from the right ventricle. Cell lysis was done using Pharm Lyse (BD, Franklin Lakes, USA), and remaining lysis buffer was removed by washing with Hank's buffered salt solution containing 5 μM ethylenediaminetetraacetic acid and 0.5% bovine serum albumin. Hepatic leukocytes were isolated, and flow cytometry and intracellular flow cytometric analysis were done as described before.[8] For details on the procedure, see Supporting Information section 10 (Figure S21). Murine macrophages were isolated from minced and collagenase-treated liver by magnetic bead separation using biotinylated anti-F4/80 antibody and streptavidin-coated magnetobeads (Miltenyi Biotech, Bergisch Gladbach, Germany). To isolate KC and iMΦ, cells were stained using antibodies and sorting was performed using a FACSAria II cell sorter (BD, Franklin Lakes, USA) as reported earlier.[36]

Gene Expression Analysis. Liver pieces were snap-frozen in liquid nitrogen, RNA was purified using the peqGold kit (PEQLAB Biotechnologie GmbH, Erlangen, Germany), and complementary DNA was generated from RNA using the First Strand cDNA synthesis kit (Roche, Penzberg, Germany). Quantitative real-time polymerase chain reaction was done based on SYBR Green Reagent (Roche, Penzberg, Germany). Reactions were done as triplicates, and β-actin was used to normalize gene expression. Primer sequences are available upon request.

Hydroxyproline and Cytokine Measurements. The hepatic hydroxyproline content that reflects the portion of total collagen was quantified as shown before.[8] Cytokine measurements of serum and liver for CCL2, CXCL1, and IL6 were done using the FlowCytomix system (eBioscience, San Diego, CA, USA).

Statistical Analysis. Statistical analysis was performed using Graph Pad Prism 4.0 (LaJolla, California, USA). Unpaired *t* tests were performed to test significance of differences between experimental groups. *P* values below 0.05 were considered as statistically significant.

Conflict of Interest: The authors declare no competing financial interest.

Acknowledgment. This work was supported by the German Research Foundation (DFG Ta434/2-1 to F.T., DFG SFB/TRR 57) and by the Interdisciplinary Center for Clinical Research (IZKF) Aachen. We thank Mrs. Aline Roggenkamp, Carmen Tag, and Sibille Sauer-Lehnen for excellent technical support.

Supporting Information Available: Detailed experimental procedures and supplemental Figures 1−21. This material is available free of charge *via* the Internet at http://pubs.acs.org.

REFERENCES AND NOTES

1. Khlebtsov, N.; Dykman, L. Biodistribution and Toxicity of Engineered Gold Nanoparticles: A Review of *In Vitro* and *In Vivo* Studies. *Chem. Soc. Rev.* **2011**, *40*, 1647–1671.

2. Longmire, M.; Choyke, P. L.; Kobayashi, H. Clearance Properties of Nano-sized Particles and Molecules as Imaging Agents: Considerations and Caveats. *Nanomedicine* **2008**, *3*, 703–717.
3. Gore, C. *Viral Hepatitis: Global Policy*; World Hepatitis Alliance, 2011.
4. Fung, J.; Lai, C. L.; Yuen, M. F. Hepatitis B and C Virus-Related Carcinogenesis. *Clin. Microbiol. Infect.* **2009**, *15*, 964–970.
5. Ioannou, G. N.; Boyko, E. J.; Lee, S. P. The Prevalence and Predictors of Elevated Serum Aminotransferase Activity in the United States in 1999−2002. *Am. J. Gastroenterol.* **2006**, *101*, 76–82.
6. Bilzer, M.; Roggel, F.; Gerbes, A. L. Role of Kupffer Cells in Host Defense and Liver Disease. *Liver Int.* **2006**, *26*, 1175–1186.
7. Bastus, N. G.; Sanchez-Tillo, E.; Pujals, S.; Farrera, C.; Lopez, C.; Giralt, E.; Celada, A.; Lloberas, J.; Puntes, V. Homogeneous Conjugation of Peptides onto Gold Nanoparticles Enhances Macrophage Response. *ACS Nano* **2009**, *3*, 1335–1344.
8. Karlmark, K. R.; Weiskirchen, R.; Zimmermann, H. W.; Gassler, N.; Ginhoux, F.; Weber, C.; Merad, M.; Luedde, T.; Trautwein, C.; Tacke, F. Hepatic Recruitment of the Inflammatory Gr1+ Monocyte Subset upon Liver Injury Promotes Hepatic Fibrosis. *Hepatology* **2009**, *50*, 261–274.
9. Zimmermann, H. W.; Tacke, F. Modification of Chemokine Pathways and Immune Cell Infiltration as a Novel Therapeutic Approach in Liver Inflammation and Fibrosis. *Inflammation Allergy: Drug Targets* **2011**, *10*, 509–536.
10. Raes, G.; Van den Bergh, R.; De Baetselier, P.; Ghassabeh, G. H.; Scotton, C.; Locati, M.; Mantovani, A.; Sozzani, S. Arginase-1 and Ym1 Are Markers for Murine, but not Human, Alternatively Activated Myeloid Cells. *J. Immunol.* **2005**, *174*, 6561author reply 6561−6562.
11. Tacke, F.; Randolph, G. J. Migratory Fate and Differentiation of Blood Monocyte Subsets. *Immunobiology* **2006**, *211*, 609–618.
12. Herbert, D. R.; Holscher, C.; Mohrs, M.; Arendse, B.; Schwegmann, A.; Radwanska, M.; Leeto, M.; Kirsch, R.; Hall, P.; Mossmann, H.; *et al.* Alternative Macrophage Activation Is Essential for Survival during Schistosomiasis and Downmodulates T Helper 1 Responses and Immunopathology. *Immunity* **2004**, *20*, 623–635.
13. Veeranarayanan, S.; Cheruvathoor Poulose, A.; Mohamed, S.; Aravind, A.; Nagaoka, Y.; Yoshida, Y.; Maekawa, T.; Kumar, D. S. FITC Labeled Silica Nanoparticles as Efficient Cell Tags: Uptake and Photostability Study in Endothelial Cells. *J. Fluoresc.* **2011**, *22*, 537–548.
14. Leonov, A. P.; Zheng, J.; Clogston, J. D.; Stern, S. T.; Patri, A. K.; Wei, A. Detoxification of Gold Nanorods by Treatment with Polystyrenesulfonate. *ACS Nano* **2008**, *2*, 2481–2488.
15. Sadauskas, E.; Wallin, H.; Stoltenberg, M.; Vogel, U.; Doering, P.; Larsen, A.; Danscher, G. Kupffer Cells Are Central in the Removal of Nanoparticles from the Organism. *Part. Fibre Toxicol.* **2007**, *4*, 10.
16. Bartneck, M.; Keul, H. A.; Singh, S.; Czaja, K.; Bornemann, J.; Bockstaller, M.; Moeller, M.; Zwadlo-Klarwasser, G.; Groll, J. Rapid Uptake of Gold Nanorods by Primary Human Blood Phagocytes and Immunomodulatory Effects of Surface Chemistry. *ACS Nano* **2010**, *4*, 3073–3086.
17. Madala, S. K.; Edukulla, R.; Davis, K. R.; Schmidt, S.; Davidson, C.; Kitzmiller, J. A.; Hardie, W. D.; Korfhagen, T. A. Resistin-like Molecule Alpha1 (Fizz1) Recruits Lung Dendritic Cells without Causing Pulmonary Fibrosis. *Respir. Res.* **2012**, *13*, 51.
18. Arredouani, M. S.; Franco, F.; Imrich, A.; Fedulov, A.; Lu, X.; Perkins, D.; Soininen, R.; Tryggvason, K.; Shapiro, S. D.; Kobzik, L. Scavenger Receptors SR-AI/II and MARCO Limit Pulmonary Dendritic Cell Migration and Allergic Airway Inflammation. *J. Immunol.* **2007**, *178*, 5912–5920.
19. Palecanda, A.; Kobzik, L. Receptors for Unopsonized Particles: The Role of Alveolar Macrophage Scavenger Receptors. *Curr. Mol. Med.* **2001**, *1*, 589–595.
20. Lipsky, P. E.; Hirohata, S.; Jelinek, D. F.; McAnally, L.; Splawski, J. B. Regulation of Human B Lymphocyte Responsiveness. *Scand. J. Rheumatol. Suppl.* **1988**, *76*, 229–235.
21. Ogura, Y.; Sutterwala, F. S.; Flavell, R. A. The Inflammasome: First Line of the Immune Response to Cell Stress. *Cell* **2006**, *126*, 659–662.
22. Huang, X.; Peng, X.; Wang, Y.; Shin, D. M.; El-Sayed, M. A.; Nie, S. A Reexamination of Active and Passive Tumor Targeting by Using Rod-Shaped Gold Nanocrystals and Covalently Conjugated Peptide Ligands. *ACS Nano* **2010**, *4*, 5887–5896.
23. Jaziri, M.; Migliore-Samour, D.; Casabianca-Pignede, M. R.; Keddad, K.; Morgat, J. L.; Jolles, P. Specific Binding Sites on Human Phagocytic Blood Cells for Gly-Leu-Phe and Val-Glu-Pro-Ile-Pro-Tyr, Immunostimulating Peptides from Human Milk Proteins. *Biochim. Biophys. Acta* **1992**, *1160*, 251–261.
24. Gref, R.; Minamitake, Y.; Peracchia, M. T.; Trubetskoy, V.; Torchilin, V.; Langer, R. Biodegradable Long-Circulating Polymeric Nanospheres. *Science* **1994**, *263*, 1600–1603.
25. Fujiu, K.; Manabe, I.; Nagai, R. Renal Collecting Duct Epithelial Cells Regulate Inflammation in Tubulointerstitial Damage in Mice. *J. Clin. Invest.* **2011**, *121*, 3425–3441.
26. Prokop, S.; Heppner, F. L.; Goebel, H. H.; Stenzel, W. M2 Polarized Macrophages and Giant Cells Contribute to Myofibrosis in Neuromuscular Sarcoidosis. *Am. J. Pathol.* **2011**, *178*, 1279–1286.
27. Sato, K.; Imai, Y.; Higashi, N.; Kumamoto, Y.; Onami, T. M.; Hedrick, S. M.; Irimura, T. Lack of Antigen-Specific Tissue Remodeling in Mice Deficient in the Macrophage Galactose-Type Calcium-Type Lectin 1/CD301a. *Blood* **2005**, *106*, 207–215.
28. Bartneck, M.; Keul, H. A.; Wambach, M.; Bornemann, J.; Gbureck, U.; Chatain, N.; Neuss, S.; Tacke, F.; Groll, J.; Zwadlo-Klarwasser, G. Effects of Nanoparticle Surface Coupled Peptides, Functional Endgroups and Charge on Intracellular Distribution and Functionality of Human Primary Reticuloendothelial Cells. *Nanomedicine* **2012**, Mar 7 [Epup ahead of print] .
29. Friedman, S. L. Molecular Regulation of Hepatic Fibrosis, an Integrated Cellular Response to Tissue Injury. *J. Biol. Chem.* **2000**, *275*, 2247–2250.
30. Mizuhara, H.; O'Neill, E.; Seki, N.; Ogawa, T.; Kusunoki, C.; Otsuka, K.; Satoh, S.; Niwa, M.; Senoh, H.; Fujiwara, H. T Cell Activation-Associated Hepatic Injury: Mediation by Tumor Necrosis Factors and Protection by Interleukin 6. *J. Exp. Med.* **1994**, *179*, 1529–1537.
31. Jenkins, S. J.; Ruckerl, D.; Cook, P. C.; Jones, L. H.; Finkelman, F. D.; van Rooijen, N.; MacDonald, A. S.; Allen, J. E. Local Macrophage Proliferation, Rather than Recruitment from the Blood, Is a Signature of TH2 Inflammation. *Science* **2011**, *332*, 1284–1288.
32. Mosser, D. M.; Edwards, J. P. Exploring the Full Spectrum of Macrophage Activation. *Nat. Rev. Immunol.* **2008**, *8*, 958–969.
33. Gordon, S.; Martinez, F. O. Alternative Activation of Macrophages: Mechanism and Functions. *Immunity* **2010**, *32*, 593–604.
34. Schumann, J.; Wolf, D.; Pahl, A.; Brune, K.; Papadopoulos, T.; van Rooijen, N.; Tiegs, G. Importance of Kupffer Cells for T-Cell-Dependent Liver Injury in Mice. *Am. J. Pathol.* **2000**, *157*, 1671–1683.
35. Loening, A. M.; Gambhir, S. S. AMIDE: A Free Software Tool for Multimodality Medical Image Analysis. *Mol. Imaging* **2003**, *2*, 131–137.
36. Heymann, F.; Hammerich, L.; Storch, D.; Bartneck, M.; Huss, S.; Russeler, V.; Gassler, N.; Lira, S. A.; Luedde, T.; Trautwein, C.; *et al.* Hepatic Macrophage Migration and Differentiation Critical for Liver Fibrosis Is Mediated by the Chemokine Receptor C-C Motif Chemokine Receptor 8 in Mice. *Hepatology* **2012**, *55*, 898–909.